

Novel Polaron State for Single Impurity in a Bosonic Mott Insulator

Yasuyuki Kato¹, K. A. Al-Hassanieh¹, A. E. Feiguin², Eddy Timmermans¹, and C. D. Batista¹

¹Theoretical Division, Los Alamos National Laboratory, Los Alamos, New Mexico 87545, USA and

² Department of Physics and Astronomy, University of Wyoming, Laramie, WY 82071, USA

(Dated: November 1, 2011)

We show that a single impurity embedded in a cold atom bosonic Mott insulator leads to a novel polaron that exhibits correlated motion with an effective mass and a linear size that nearly diverge at critical value of the on-site impurity-boson interaction strength. Cold atom technology can tune the polaron's properties and break up the composite particle into a deconfined impurity-hole and boson particle state at finite, controllable polaron momentum.

PACS numbers: Valid PACS appear here

The exploration of and unprecedented control over quantum many-body systems have become central driving forces in cold-atom physics. Optical lattices (the standing wave patterns of frequency-stable, reflected laser beams that are experienced by ultra-cold atoms as periodic potentials [1]) have unlocked strongly-correlated lattice physics to cold atom simulation. The Bose-Hubbard Hamiltonian [2] has successfully and quantitatively modeled boson atom dynamics in such optical lattices. Studies of the boson superfluid to Mott insulator (MI) phase transition predicted within the Bose-Hubbard model [3] highlight the unusual cold atom access and control: experiments observed the transition [4], revivals of inter-site superfluid coherence [5] and different integer filling-number islands in the MI phase as seen spectroscopically [6] and, more recently, by direct imaging [7–10]. In this Letter, we show that by combining the control over optical lattice parameters (varying the barrier height), over the inter-particle interactions (varying an external, homogeneous magnetic field in a Feshbach resonance [11, 12]), and over particle-species (creating mixtures of distinguishable kinds of atoms), cold atom experiments can realize a novel [18] and controllable polaron in the MI phase.

The polaron state is induced by an impurity atom that experiences the same (or similar) optical lattice potential as the MI bosons from which it is distinguishable. The polaron consists of the impurity and a boson that is promoted to the next Hubbard band by a strong impurity-boson repulsion. If the impurity-boson interaction is Feshbach tuned to be nearly as repulsive as the boson-boson interaction, the excited boson remains pinned to the impurity site. The boson-impurity pair propagates through the lattice with finite total momentum \mathbf{K} . The linear polaron size, $\lambda_{\mathbf{K}}$, or average distance between the impurity and the excited boson sensitively depends on \mathbf{K} , and increases with increasing impurity-boson repulsive interaction U_{IB} [19]. Surprisingly, *the effective mass of the polaron increases with its size*. Moreover, in the strong coupling limit the effective mass diverges at the critical value of U_{IB} above which the boson-impurity pair becomes unbound ($\lambda_0 \rightarrow \infty$). Most significantly, optical lattice experiments can create probe and manipulate composite particles with properties that are unusual in

traditional polaronic and excitonic systems.

We will model our problem with a bosonic Hubbard Hamiltonian on a hyper-cubic lattice of dimension d :

$$\mathcal{H} = -t_B \sum_{\langle \mathbf{r}, \mathbf{r}' \rangle} b_{\mathbf{r}}^\dagger b_{\mathbf{r}'} - t_I \sum_{\langle \mathbf{r}, \mathbf{r}' \rangle} c_{\mathbf{r}}^\dagger c_{\mathbf{r}'} + \frac{U_{BB}}{2} \sum_{\mathbf{r}} b_{\mathbf{r}}^\dagger b_{\mathbf{r}}^\dagger b_{\mathbf{r}} b_{\mathbf{r}} + U_{IB} \sum_{\mathbf{r}} b_{\mathbf{r}}^\dagger b_{\mathbf{r}} c_{\mathbf{r}}^\dagger c_{\mathbf{r}}. \quad (1)$$

The operator $b_{\mathbf{r}}^\dagger$ ($b_{\mathbf{r}}$) creates (annihilates) a boson on site \mathbf{r} , while $c_{\mathbf{r}}^\dagger$ ($c_{\mathbf{r}}$) creates (annihilates) the impurity. $\langle \mathbf{r}, \mathbf{r}' \rangle$ indicates that \mathbf{r} and \mathbf{r}' are nearest-neighbors. The statistics of $c_{\mathbf{r}}^\dagger$ and $c_{\mathbf{r}}$ is irrelevant because we are considering a *single* impurity problem.

Here we will only consider the case of strongly repulsive on-site boson-boson interaction, $U_{BB} \gg n|t_B|, |t_I|$, and integer filling factor $\langle b_{\mathbf{r}}^\dagger b_{\mathbf{r}} \rangle = n$ to stabilize the MI state. An increase in the intensity of the optical lattice laser of wavelength λ so that the lattice height V_0 significantly exceeds the recoil energy $\hbar\omega_R$ ($= \hbar^2/[2m_B\lambda^2]$), where m_B is the actual boson mass) drives the boson system deep into the MI regime. This increase tightens the trapping frequency ω_T of the optical lattice wells, $\omega_T = 2\omega_R\sqrt{x}$, where $x = V_0/\hbar\omega_R$. For fixed boson-boson scattering length a_{BB} , an increase in x , $x > 1$, enhances $U_{BB} \approx \hbar\omega_T\sqrt{8\pi}(a_{BB}/\lambda)x^{1/4}$, and exponentially decreases the hopping matrix element t_{BB} which we estimate as $t_B \approx (3/2)\hbar\omega_T e^{-(\pi/2)^2\sqrt{x}}$. Scattering lengths take the value of a few nm whereas the optical wavelength is of order of a micron but even for $x \sim 9$, U_{BB} can exceed t_B by an order of magnitude whereas t_B can still be of the order of 10 Hz. Thus, the MI-regime can be accessed by varying the optical lattice height, which leaves a homogeneous magnetic field tuned near a Feshbach resonant value as a control knob to vary a_{BB} ($\propto U_{BB}$) or the impurity-boson scattering length a_{IB} ($\propto U_{IB}$) independently. We consider the regime $U_{IB} \gg n|t_B|, |t_I|$. The eigenstates of \mathcal{H} become highly degenerate in the static limit $t_B = t_I = 0$. The lowest-energy eigenstates, illustrated in Fig.1, can be expressed as

$$|\mathbf{R}, \mathbf{r}\rangle = \frac{1}{\sqrt{n(n+1)}} c_{\mathbf{R}}^\dagger b_{\mathbf{R}+\mathbf{r}}^\dagger b_{\mathbf{R}} |0\rangle \text{ for } \mathbf{r} \neq \mathbf{0}, \quad (2)$$

$$|\mathbf{R}, \mathbf{0}\rangle = c_{\mathbf{R}}^\dagger |0\rangle, \quad (3)$$

where $|0\rangle = \prod_{\mathbf{r}} (n!)^{-1/2} b_{\mathbf{r}}^{\dagger n} |\emptyset\rangle$, and where $|\emptyset\rangle$ denotes the vacuum state. The states $|\mathbf{R}, \mathbf{r}\rangle$ correspond to the impurity at site \mathbf{R} creating a hole at the same site and relocating the removed boson to site \mathbf{r} (see Fig. 1(a)). The size of the resulting polaron is the size of the particle-hole bound state, i.e., the mean value of \mathbf{r} .

The energy eigenvalues of the states (3) are given by

$$\begin{aligned}\mathcal{H}|\mathbf{R}, \mathbf{r}\rangle &= (U_{BB} + U_{IB}(n-1) + E_0)|\mathbf{R}, \mathbf{r}\rangle \text{ for } \mathbf{r} \neq \mathbf{0} \\ \mathcal{H}|\mathbf{R}, \mathbf{0}\rangle &= (nU_{IB} + E_0)|\mathbf{R}, \mathbf{0}\rangle\end{aligned}\quad (4)$$

where $E_0 = NU n(n-1)/2$ represents the ground state energy of the undoped MI: $\mathcal{H}|0\rangle = E_0|0\rangle$ (N is the total number of lattice sites). The energy of any other eigenstate is of order U_{BB} or U_{IB} higher than the energy of the eigenstates (4). According to perturbation theory, to lowest order in the small parameters t_{ν}/U_{BB} and t_{ν}/U_{IB} ($\nu = I, B$), we can exclude those high-energy states and restrict the action of \mathcal{H} to the lowest energy subspace generated by the states (4). In this way we reduce the many-body problem to a two-body system described by the low-energy effective Hamiltonian,

$$\begin{aligned}\bar{\mathcal{H}} &= \sum_{\mathbf{K}} \bar{\mathcal{H}}_{0\mathbf{K}} + \bar{\mathcal{H}}_{1\mathbf{K}}, \\ \bar{\mathcal{H}}_{0\mathbf{K}} &= -t_B(n+1) \sum_{\langle \mathbf{r}, \mathbf{r}' \rangle} |\mathbf{K}, \mathbf{r}\rangle \langle \mathbf{K}, \mathbf{r}'|, \\ \bar{\mathcal{H}}_{1\mathbf{K}} &= \frac{\tau}{\sqrt{2d}} \sum_{\langle \mathbf{0}, \mathbf{r}' \rangle} (|\mathbf{K}, \mathbf{0}\rangle \langle \mathbf{K}, \mathbf{r}'| + |\mathbf{K}, \mathbf{r}'\rangle \langle \mathbf{K}, \mathbf{0}|) \\ &\quad + U_{\mathbf{K}} |\mathbf{K}, \mathbf{0}\rangle \langle \mathbf{K}, \mathbf{0}|,\end{aligned}\quad (5)$$

where $\tau = t_B \sqrt{2d} [n+1 - \sqrt{n(n+1)}]$,

$$U_{\mathbf{K}} = U_{IB} - U_{BB} + \epsilon_{\mathbf{K}}^I, \quad \epsilon_{\mathbf{K}}^I = -t_I \sum_{\langle \mathbf{0}, \mathbf{r}' \rangle} e^{i\mathbf{K} \cdot \mathbf{r}'}, \quad (6)$$

and

$$\begin{aligned}|\mathbf{K}, \mathbf{r}\rangle &= \frac{1}{\sqrt{Nn(n+1)}} \sum_{\mathbf{R}} e^{i\mathbf{K} \cdot \mathbf{R}} c_{\mathbf{R}}^{\dagger} b_{\mathbf{R}+\mathbf{r}}^{\dagger} b_{\mathbf{R}} |\emptyset\rangle \text{ for } \mathbf{r} \neq \mathbf{0}, \\ |\mathbf{K}, \mathbf{0}\rangle &= \frac{1}{\sqrt{N}} \sum_{\mathbf{R}} e^{i\mathbf{K} \cdot \mathbf{R}} c_{\mathbf{R}}^{\dagger} |\emptyset\rangle = c_{\mathbf{K}}^{\dagger} |\emptyset\rangle.\end{aligned}\quad (7)$$

\mathbf{K} is the center-of-mass momentum of the effective two-particle system. Since \mathbf{K} is a conserved quantity, the states with a given \mathbf{K} generate an invariant subspace of $\bar{\mathcal{H}}$ leading to an effective single-particle problem in the relative coordinate \mathbf{r} . This effective particle moves in a \mathbf{K} dependent central potential given by $V(\mathbf{r}) = U_{\mathbf{K}} \delta_{\mathbf{r}, \mathbf{0}}$. The hopping amplitude is $(n+1)t_B$ except for bonds containing the origin where it is equal to $\sqrt{n(n+1)}t_B$. In an optical lattice, the impurity atom can be accelerated with forces that are invisible to the b -bosons by using the recently demonstrated species-specific dipole potentials. [13, 14]

One-Dimensional Case. Since the potential $V(\mathbf{r})$ can be attractive, we look for bound-state solutions of $\bar{\mathcal{H}}_{\mathbf{K}}$.

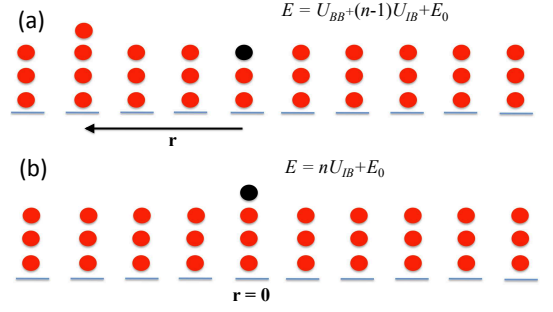


FIG. 1: (color online) Lowest energy eigenstates of a MI with n bosons per site ($n = 3$ in the figure) doped with a single impurity (black particle). (a) The “particle” and the “hole” occupy different positions and the vector \mathbf{r} is the relative position. (b) The “particle” and the “hole” occupy the same position ($\mathbf{r} = \mathbf{0}$).

For $d = 1$, the exact ground state of $\bar{\mathcal{H}}_{\mathbf{K}}$ can be expressed as

$$|\psi_{\mathbf{K}}^0\rangle = \alpha_{\mathbf{K}} \left[\frac{(n+1)}{\sqrt{n(n+1)}} |\mathbf{K}, \mathbf{0}\rangle + \sum_{\mathbf{r} \neq \mathbf{0}} e^{-r/\lambda_{\mathbf{K}}} |\mathbf{K}, \mathbf{r}\rangle \right], \quad (8)$$

with $\alpha_{\mathbf{K}}^2 = n(1 - e^{-1/\lambda_{\mathbf{K}}}) / (1 + n - e^{-1/\lambda_{\mathbf{K}}})$, and

$$e^{1/\lambda_{\mathbf{K}}} = -\frac{U_{\mathbf{K}}}{2t_B(n+1)} + \sqrt{\frac{U_{\mathbf{K}}^2}{4t_B^2(n+1)^2} + \frac{(n-1)}{(n+1)}}. \quad (9)$$

The corresponding eigenvalue is

$$\epsilon_{\mathbf{K}}^b = -2t_B(n+1) \cosh(1/\lambda_{\mathbf{K}}). \quad (10)$$

This equation has a physical solution ($\lambda_{\mathbf{K}} > 0$) for $U_{\mathbf{K}} < U_c$ with $U_c = -2t_B$:

$$\lambda_{\mathbf{K}} = \frac{2t_B n}{U_c - U_{\mathbf{K}}}. \quad (11)$$

Note that the size of the polaron, λ_0 , diverges for $U_0 \rightarrow U_c$. The solutions for $U_{\mathbf{K}} > U_c$ are unbound particle-hole states: the impurity-hole item and the boson that was promoted to the next Hubbard band propagate independently while scattering in each other's vicinity.

The attractive potential $U_{\mathbf{K}}$ has to reach a critical value for the stabilization of the bound state because the hopping amplitude is smaller for the bonds that include the origin. Since we are assuming that $t_I, t_B > 0$, $\epsilon_{\mathbf{K}}^0$ has its minimum at $\mathbf{K} = \mathbf{0}$. The effective mass, m_I^* , of the exciton is given by the equation:

$$\frac{1}{m^*} \equiv \partial_{\mathbf{k}}^2 \epsilon_{\mathbf{K}}^b |_{\mathbf{K}=\mathbf{0}} = \frac{|\langle \psi_{\mathbf{0}}^0 | \mathbf{K}, \mathbf{0} \rangle|^2}{m_I} \quad (12)$$

where $m_I = (2|t_I|)^{-1}$ is the bare (lattice) mass of the impurity in units in which the unit length is given by the lattice constant and $\hbar = 1$. The identity (12) follows from the Hellmann-Feynman theorem and $\partial_{\mathbf{K}} \langle \psi_{\mathbf{K}}^0 | \mathbf{K}, \mathbf{0} \rangle |_{\mathbf{K}=\mathbf{0}} = 0$. By taking the large λ_0 limit, we

obtain the relation between m^*/m_I and λ_0 near the critical point:

$$\frac{m^*}{m_I} = \frac{n\lambda_0}{n+1}. \quad (13)$$

In the strong coupling regime the effective mass of the MI impurity polaron is proportional to its size. This behavior, very different from that of lattice polarons induced by electrons in condensed matter, is caused by the unusual mode of transportation: the impurity can hop only when the displaced boson and the hole mutually annihilate ($\mathbf{r}=0$). As a consequence of this correlated motion, the effective mass is proportional to $|\langle\psi_0^0|\mathbf{K}, \mathbf{0}\rangle|^2$ (see Eq.(12)).

To test the validity of $\bar{\mathcal{H}}$ we computed the correlation function $C_{ID}(\mathbf{r})$ between the positions of the impurity and the site with one additional boson by solving the original Hubbard model with the constraint of no more than two bosons per site. We used the Density-Matrix Renormalization Group (DMRG)[15, 16]. Figure 2 shows the comparison between the numerical results for a chain of $L = 40$ sites and the analytical results given by Eq.(8). The upper curves correspond to $U_{IB} = U_{BB} + t_B$ and the lower ones correspond to $U_{IB} = U_{BB} - 2t_B$. As expected, both results coincide in the strong-coupling limit. Note that the extra boson is displaced over only a few lattice sites ($r \leq 6$), so that this physics can be realized in today's optical lattices which typically have a linear size corresponding to 100 sites or so.

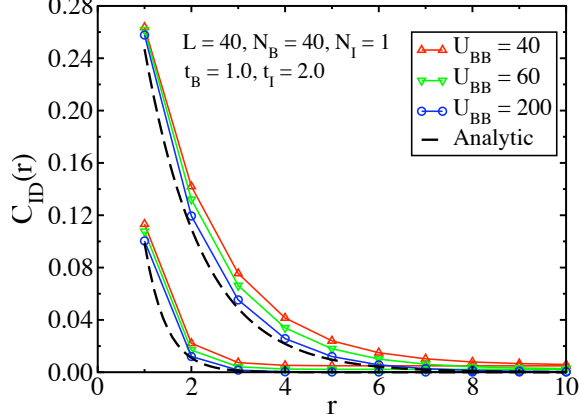


FIG. 2: (color online) Correlation function between the positions of the impurity and the site with one additional boson for $n = 1$. The dashed line is the analytical result of Eq.(8). The full lines were obtained by solving \mathcal{H} (with a constraint of no more than two particles per site) by means of the DMRG method in a chain of $L = 40$ sites. The upper (lower) curves correspond to $U_{IB} = U_{BB} + t_B$ ($U_{IB} = U_{BB} - 2t_B$).

General Case. The bound states of $\bar{\mathcal{H}}$ can be found in any dimension by using the Green's function formalism [17]. We construct a basis of states that diagonalizes $\bar{\mathcal{H}}_{1\mathbf{K}}$ and we separate $\bar{\mathcal{H}}_{\mathbf{K}}$ into three terms, $\bar{\mathcal{H}}_{\mathbf{K}} = \bar{\mathcal{H}}_{0\mathbf{K}} + \bar{\mathcal{H}}_{\mathbf{K}}^+ + \bar{\mathcal{H}}_{\mathbf{K}}^-$, where

$$\bar{\mathcal{H}}_{\mathbf{K}}^{\pm} = \epsilon^{\pm}|\mathbf{K}, \psi^{\pm}\rangle\langle\mathbf{K}, \psi^{\pm}|, \quad (14)$$

$$\epsilon^{\pm} = (U_{\mathbf{K}} \pm \zeta_{\mathbf{K}})/2, \quad \zeta_{\mathbf{K}} = \sqrt{U_{\mathbf{K}}^2 + 4\tau^2},$$

$$|\mathbf{K}, \psi^{\pm}\rangle = u_{\mp}|\mathbf{K}, \mathbf{0}\rangle \mp u_{\pm}|\psi_s\rangle, \quad |\psi_s\rangle = \frac{1}{\sqrt{Z}} \sum_{\langle\mathbf{0}, \mathbf{r}'\rangle} |\mathbf{K}, \mathbf{r}'\rangle,$$

and $u_{\pm} = (1 \pm U_{\mathbf{K}}/\zeta_{\mathbf{K}})^{1/2}/\sqrt{2}$. By introducing the Green operators

$$\begin{aligned} G_{\mathbf{K}}^0(z) &\equiv \frac{1}{z - \bar{\mathcal{H}}_{0\mathbf{K}}}, \quad G_{\mathbf{K}}^+(z) \equiv \frac{1}{z - \bar{\mathcal{H}}_{0\mathbf{K}} - \bar{\mathcal{H}}_{\mathbf{K}}^+}, \\ G_{\mathbf{K}}(z) &\equiv \frac{1}{z - \bar{\mathcal{H}}_{\mathbf{K}}}, \end{aligned} \quad (15)$$

we obtain the $G_{\mathbf{K}}^+(z)$ -operator from $G_{\mathbf{K}}^0(z)$ by expanding in $\bar{\mathcal{H}}_{\mathbf{K}}^+$:

$$G_{\mathbf{K}}^+ = G_{\mathbf{K}}^0 + G_{\mathbf{K}}^0|\mathbf{K}, \psi^+\rangle \frac{\epsilon^+}{1 - \epsilon^+ G_{\mathbf{K}}^0(\psi^+, \psi^+)} \langle\mathbf{K}, \psi^+| G_{\mathbf{K}}^0$$

with $G_{\mathbf{K}}^0(\psi^+, \psi^+) = \langle\mathbf{K}, \psi^+| G_{\mathbf{K}}^0|\mathbf{K}, \psi^+\rangle$. Similarly, by considering $\bar{\mathcal{H}}_{\mathbf{K}}^+$ as the unperturbed Hamiltonian and expanding in the perturbation $\bar{\mathcal{H}}_{\mathbf{K}}^-$, we find

$$G_{\mathbf{K}} = G_{\mathbf{K}}^+ + G_{\mathbf{K}}^+|\mathbf{K}, \psi^-\rangle \frac{\epsilon^-}{1 - \epsilon^- G_{\mathbf{K}}^+(\psi^-, \psi^-)} \langle\mathbf{K}, \psi^-| G_{\mathbf{K}}^+, \quad (16)$$

with $G_{\mathbf{K}}^+(\psi^-, \psi^-) = \langle\mathbf{K}, \psi^-| G_{\mathbf{K}}^+|\mathbf{K}, \psi^-\rangle$. The exact dispersion relation of the bound state is obtained from the poles of $G_{\mathbf{K}}(\mathbf{0}, \mathbf{0}) \equiv \langle\mathbf{K}, \mathbf{0}| G_{\mathbf{K}}|\mathbf{K}, \mathbf{0}\rangle$.

We consider $\epsilon_{\mathbf{K}}^b$, λ_0 and m^* near the critical point, $U_0 = U_c$. Identifying $\lambda_{\mathbf{K}}$ in d -dimensions from the asymptotic behavior of the bound state wave function: $\langle\psi_{\mathbf{K}}^0|\mathbf{K}, \mathbf{r}\rangle \sim e^{-r/\lambda_{\mathbf{K}}}/r^{(d-1)/2}$ for $\mathbf{r} = (r, 0, 0, \dots)$ and $r \gg 1$, we obtain

$$\epsilon_{\mathbf{K}}^b = -2t_B(n+1) [d-1 + \cosh(\lambda_{\mathbf{K}}^{-1})]. \quad (17)$$

Thus, $\lambda_0 \propto \Delta_b^{-1/2}$ where $\Delta_b \equiv -2dt_B(n+1) - \epsilon_0^b$ is the composite particle binding energy. From Eq. (12), we obtain the effective mass, m^* ,

$$\frac{m_I}{m^*} = \left. \frac{d\epsilon_{\mathbf{K}}^b}{dU_{\mathbf{K}}} \right|_{\mathbf{K}=\mathbf{0}}. \quad (18)$$

Near the critical point, the large polaron size washes out the dependence on specifics that occur on the scale of the lattice constant. Hence, we expect the binding energy to vanish with the same scaling laws as the binding of a single impurity [17] [20]:

$$\begin{aligned} \Delta_b(\mathbf{0}) &\propto (U_{\mathbf{K}} - U_c)^2 \quad \text{for } d = 1 \text{ and } 3, \\ \Delta_b(\mathbf{0}) &\propto \exp\left[\frac{C}{U_0 - U_c}\right], \quad \text{for } d = 2, \end{aligned} \quad (19)$$

where the constant C depends on microscopic details of \mathcal{H} . These equations lead to the relation between m^* and

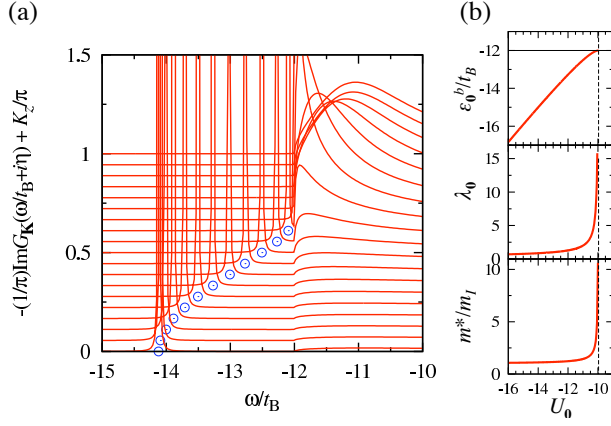


FIG. 3: (a) K_z dependence of spectral weight for the simple cubic lattice ($t_B = t_I = 1$, $n = 1$, $K_x = K_y = 0$, and $U_{BB} - U_{IB} = 7$). Each line is shifted by K_z/π for visualization. We use $\eta = 2^{-10}$ as an infinitesimal constant. (b) U_0 dependences of the bound state energy ϵ_0^b (top), linear size of the polaron λ_0 (middle), and ratio of effective and bare masses m^*/m_I (bottom) for $n=1$. The dashed line indicates $U_0 = U_c$.

λ_0 :

$$\begin{aligned} \frac{m^*}{m_I} &\propto \lambda_0 \text{ for } d = 1 \text{ and } 3, \\ \frac{m^*}{m_I} &\propto \lambda_0^2 (\ln \lambda_0)^2 m_I \text{ for } d = 2. \end{aligned}$$

For the case of a simple cubic lattice in $d=3$, Fig. 3 shows the spectral density obtained from Eq.(16). The bound states for different values of \mathbf{K} that appear below the bottom of continuum spectrum ($U_{\mathbf{K}} < U_c$) form the polaron band. U_c is obtained by finding a root of $1 - \epsilon^- G_{\mathbf{K}}^+(\psi^-, \psi^-) = 0$ at $z = -2dt_B(n+1)$ as a function of n . Figure 3(b) shows U_0 dependences of ϵ_0^b , λ_0 and m^*/m_I for $n = 1$. Note that the effective mass m^* and

the polaron size increase sharply with decreasing $U_c - U_0$. By superimposing a linear or harmonic impurity-specific potential and observing the subsequent acceleration or oscillation, cold atom experiments can measure m^* directly.

The divergence of the effective mass for $U_0 \rightarrow U_c$ is cut off at a finite value $m_{\text{max}}^* = U_{IB}/(2nt_I t_B)$ when the next order correction in t_ν/U_{IB} is included implying that m^* can be tuned over a large spectrum of values ranging from $m_I = 1/2t_I$ to $U_{IB}m_I/(2nt_B)$. On the other hand, the polaron size can be tuned from zero to infinity by changing the effective potential U_0 or, equivalently, the difference between U_{IB} and U_{BB} . Such dependence of m^* on the particle-hole pair size is not shared by the usual two-particle bound states such as condensed matter excitons. In those cases the mass of the bound state is well approximated by the sum of the masses. The Mott polaron mass increases with size because, to linear order in t_I , the impurity can only move when the particle and hole share the same site (see Fig.1(b)). This strongly correlated mechanism leads to a highly tunable m^* .

The control offered by cold atom technology over polaron size and mass hints at the intriguing prospect of studying the quantum phase transition between a “confined” gas of boson-impurity polarons and two “deconfined” gases of impurities and bosons in the next Hubbard band. The driving parameter of this transition is the difference $U_{IB} - U_{BB}$. By reducing the ratio U_{IB}/t_B , while keeping U_0 fixed, it would be possible to vary the polaron mass near the transition. The competition between potential and kinetic energies could also lead to an intermediate crystallization of polarons in the large m^* regime.

We are grateful to S. A. Trugman for many useful discussions. Work at the LANL was performed under the auspices of the U.S. DOE contract No. DE-AC52-06NA25396 through the LDRD program. A.E.F. thanks NSF for support through Grant No. DMR-0955707.

-
- [1] M. Greiner and S. Fölling, *Nature* **453**, 736 (2008).
 - [2] D. Jaksch, C. Bruder, J. I. Cirac, C. W. Gardiner, and P. Zoller, *Phys. Rev. Lett.* **81**, 3108 (1998).
 - [3] M. P. A. Fisher, P. B. Weichman, G. Grinstein, and D. S. Fisher, *Phys. Rev. B* **40**, 546 (1989).
 - [4] M. Greiner, O. Mandel, T. Esslinger, T. Hänsch, and I. Bloch, *Nature* **415**, 39 (2002).
 - [5] M. Greiner, O. Mandel, T. Hänsch, and I. Bloch, *Nature* **419**, 51 (2002).
 - [6] G. Campbell, J. Mun, M. Boyd, P. Medley, A. Leanhardt, L. Marcassa, D. Pritchard, and W. Ketterle, *Science* **313**, 649 (2006).
 - [7] W. Bakr, J. Gillen, A. Peng, S. Fölling, and M. Greiner, *Nature* **462**, 74 (2009).
 - [8] J. Sherson, C. Weitenberg, M. Endres, M. Cheneau, I. Bloch, and S. Kuhr, *Nature* pp. 68–72 (2010).
 - [9] W. Bakr, A. Peng, M. Tai, R. Ma, J. Simon, J. Gillen, S. Fölling, L. Pollet, and M. Greiner, *Science* **329**, 547 (2010).
 - [10] C.-L. Hung, X. Zhang, N. Gemelke, and C. Chin, *Phys. Rev. Lett.* **104**, 160403 (2010).
 - [11] S. Inouye, M. Andrews, J. Stenger, H. Miesner, D. Stamper-Kurn, and W. Ketterle, *Nature* **392**, 151 (1998).
 - [12] I. Bloch, J. Dalibard, and W. Zwerger, *Rev. Mod. Phys.* **80**, 885 (2008).
 - [13] J. Catani, G. Barontini, G. Lamporesi, F. Rabatti, G. Thalhammer, F. Minardi, S. Stringari, and M. Inguscio, *Phys. Rev. Lett.* **103**, 140401 (2009).
 - [14] G. Lamporesi, J. Catani, G. Barontini, Y. Nishida, M. Inguscio, and F. Minardi, *Phys. Rev. Lett.* **104**, 153202 (2010).
 - [15] S. R. White, *Phys. Rev. Lett.* **69**, 2863 (1992).
 - [16] S. R. White, *Phys. Rev. B* **48**, 10345 (1993).

- [17] E. Economou, *Green's functions in Quantum Physics* (Springer-Verlag, Berlin, 2006), 3rd ed.
- [18] The word 'novel' here refers not only to the cold atom environment but also to the properties of the polaron.
- [19] The increase in polaron size with increasing U_{IB} contrasts with the size of an impurity atom in boson superfluid
- [20] The impurity only affects the diagonal energy of the site at the origin.